

Aerodynamic Analysis of Jet-Blast using CFD considering as example a Hangar and an AIRBUS A380 configuration

S. Melber-Wilkending

German Aerospace Center (DLR)
Institute of Aerodynamics and Flow Technology
Lilienthalplatz 7, D-38108 Braunschweig, Germany

Summary

The paper describes the aerodynamic analysis of jet-blast. This so called jet-blast plays an important role for the design and the operation of airports. Below the setup and validation of a process-chain based on the DLR-TAU code with adaptation and flow solver for the determination of the jet-wake behind jet engines for viscous flows is shown. As an example the jet-blast impact on a hangar by an AIRBUS A380 configuration is simulated using this technique.

1 Introduction

For the design and operation of an airport the volume of traffic, available amount of space and legal requirements can play an important role. Also aerodynamic questions may have significant impact for ground operations. Considering as an example the introduction of the new AIRBUS A380 is considered in the following and ways to get answers on these questions using numerical flow simulation are shown.

For the operation of the apron area and runways the jet-blast is one of the limiting factors. The jet-blast is caused by highly accelerated air flow and exhaust gas behind jet engines. To prevent the hazard of persons, ground vehicles and other aircraft by jet-blast, security areas and the safe operations of taxiways have to be determined. Furthermore, the aerodynamic loads on buildings (e.g. blast-fences) caused by jet-blast and also possible additional wind-load is a priori unknown.

The strength of jet-blast behind aircrafts with jet-engines is a function of the maximum thrust of an airplane. The civil aircraft with the strongest thrust to date is the Boeing B747-400 with a maximum thrust of $4 \times 282 \text{ kN}$ is far of the maximum thrust of an as soon to be introduced AIRBUS A380 with $4 \times 340 \text{ kN}$ thrust. In the sector of twin-engines more thrust per engine is realized, e.g. $2 \times 436 \text{ kN}$ of a Boeing B777-300. This increasing thrust of modern jet-engine affects the design of buildings or the determination of security areas and leads to the inspection or modification of existing facilities at airports.

Currently only a few methods for the solution jet-blast problems are available. The methods for the prediction of jet flows used by aircraft- and engine manufactures can be used for the determination of the propagation of undisturbed jets behind engines, interactions of the jets with objects (e.g. blast-fences) are not covered by them. On the other side, experiments with existing aircrafts are too cost-intensive or, in case of aircrafts in development like the AIRBUS A380, are not possible. Also model experiments with reduced size are often suffer from considerable costs and scaling problems.

In the following the numerical flow solution (CFD) is shown as a possible alternative to address of the problem of jet-blast. For this purpose the layout and validation of a process-chain based on the DLR-TAU code is described. This process-chain has been successfully used for the inspection of blast security facilities of an international airport. Due to confidentiality restrictions the results cannot be shown here. For the demonstration of the capabilities of this technique an example of a hangar located on the apron area is shown encountered by jet-blast of an AIRBUS A380 in take-off. Further more cross-wind with 20 kts is taken into account for the simulation. The numerical investigation includes the complete aircraft configuration, the fictive hangar and apron area. Physical features like e.g. the ground effect are incorporated in the simulation.

2 Geometry

In the considered take-off case usually the complete high-lift devices (e.g. slats, flaps) of a transport aircraft are deployed. The interaction of the engine-jets with these elements or the empennage cannot be disregarded a priori. For this reason the complete high-lift configuration of the AIRBUS A380 is considered. The landing gears are included, because in the considered ground case they are not affected by the jet and thus they have no effect on the jet flow. The engines used exemplarily below are of the Trent 900 engine family with a "maximum take-off thrust" of 4 x 340 kN for the AIRBUS A380. The configuration of the AIRBUS A380 is provided by AIRBUS Germany.

The obstacle in the engine-jet of the AIRBUS A380 is a fictive hangar, consisting of the square main part with a dimension of 150 m x 85 m x 37 m. On the forefront a balustrade with a height of 10 m is added, see figure 1. The positioning of the aircraft in relation to the hangar is shown likewise in this figure.

3 Flow Solution Method

The solution of the Reynolds-averaged Navier-Stokes equations (RANS) is done using the hybrid unstructured DLR TAU-code [1]. For the solution of the viscous flow the $k - \omega$ -SST turbulence model of Menter [2] was used, which combines robustness with suitability for jet flows. The grids necessary for the discretisation of the

volume around the configuration are based on the geometry discussed in the previous section. They are built using the grid generator CENTAUR from CentaurSoft [3].

In order to reduce the number of grid points only such boundaries are simulated with a viscous boundary layer resolution for which an estimated influence on the flow field is anticipated. These are the engines including the pylons, because the jets arise from them and initial mixing processes of the fan- and core-jets can be found there. All other boundaries like wing, high-lift systems, fuselage or ground are simulated by inviscid surfaces. The aircraft except for the flaps in the engine area does not face a flow and the boundary-layer influence of parts in recumbent flow can be disregarded. At the ground and the hangar the influence of the viscosity is also small, because the interaction with the jet is impulse-dominated.

The initial hybrid unstructured grids are comparatively coarse in the area of the engine-jet. This leads to an increased numerical dissipation in these areas and with it an unphysical dissipation of the jet and smearing out of the gradients in the flow field. A general refinement is impractical because of the big volume influenced by the jet and the resulting high number of grid points. Particularly the interaction of the jet with obstacles cannot be captured with suitable discretisation. Hence automatic grid adaptation is used, based on the flow solution of the initial grid using gradients of flow variables for a local grid refinement.

The disadvantage of adaptive grid refinement used at long-range flow phenomena like engine jets is the slow propagation of the increased grid resolution in the area of the coarse grid. The reason is that the gradient sensors respond only weakly in the coarse grid because of the numerical dissipation and the smeared out flow solution. This behavior can be improved by using a multiple adaptation - a so called adaptation-chain.

The gradient sensor used for the jet adaptation is the total pressure loss, because inside the jet a pressure gain can be found whereas in the partly stagnated flow around the jet a total pressure loss takes place. In the area between both significant gradients can be found which lead to an increased grid resolution there by grid adaptation. To resolve the interaction of the jet with obstacles by grid adaptation the total pressure loss is not well suited because of its small value there. Using an speed-sensor based on the absolute value of the flow velocity in combination with the total pressure loss sensor improves this situation.

4 Results

4.1 Comparison of numerical results with reference methods

For the comparison of the numerical simulation of jet flows behind jet-engines with other methods reference-data of AIRBUS [4] as well as analytical results of an axisymmetric free jet in turbulent flow [5] are used. The data for comparison were analyzed concerning uncertainties and model assumptions and compared to CFD-simulations of an isolated jet-engine to demonstrate the applicability of the DLR TAU-code for the task "ground simulation".

As one example in figure 2 the lines of constant velocity of the analytical data and the numerical simulation of an isolated jet-engine for a thrust of 340 kN and 391 kN are compared. Whereas in figure 3 the reference-data used by AIRBUS for a thrust of 340 kN per engine is shown. Comparing both figures the increased jet range for the lines of constant velocity $|V| = 46 \text{ m/s}$ (17 %) and $|V| = 30 \text{ m/s}$ (30 %) of the reference-data can be found, whereas the lines of constant velocity $|V| = 15 \text{ m/s}$ has more range in the numerical simulation. The differences can be attributed on the different number of engines: one in the numerical simulation and two in the reference-data of AIRBUS.

In figure 2 additive to the lines of constant velocity of 340 kN thrust also the lines of constant velocity of 391 kN thrust are shown. The by 15% increased thrust can be used to determine the sensitivity of the flow field to the thrust. Compared to the results of the numerical simulation at 340 kN thrust an increased jet range can be found as expected. In figure 2 further more the analytical results are depicted. There a slightly reduced extension is found for all lines of constant velocity. The reason is mainly the assumption of a constant viscosity in the complete flow field in the derivation of the analytical model.

Altogether the comparisons of the numerical simulation to other methods shows the applicability of the choosen method DLR TAU-code for the task "jet-blast". Limiting assumptions necessary in the reference-data or the analytical method can be omitted in the RANS simulations.

4.2 Configuration AIRBUS 380 / Hangar

In this section the numerical results of the simulation of an AIRBUS A380 in take-off configuration including a hangar and the ground presence are shown and discussed. A thrust of 4 x 340 kN and a wind with 20 kts and a direction of 20° to the aircraft center-line are used for the simulation.

To show the complete flow field in a three-dimensional view in figure 4 (left) the area of constant velocity of $|V| = 15 \text{ m/s}$ is depicted. In this figure the process of jet-flow mixing of the engines of the left / right wing can be seen: In the area of the elevator the jets are already mixed. At the impinging on the hangar the jets of the right wing evade laterally and turn upwards. Behind the hangar the jets flow off in one front. A significant influence of the cross wind cannot be found.

Important for the operation of an aircraft is the avoidance of recirculation, so that exhaust gas can re-enter in the inlet of an jet engine. Based on the shown area of constant velocity this effect cannot be found in the presented configuration.

To determine security areas, both around the hangar and the aircraft, the velocity distribution directly above the ground is accounted for. In figure 4(right) flow velocities of $|V| \geq 15 \text{ m/s}$ are depicted. Beside the trace of the jet behind the aircraft to the hangar the raise and lateral deflection of the jet starting from the left wing can be clearly seen. Furthermore a part of the flow is deflected on the front of the hangar. For the definition of security areas against jet-blast on the apron limiting flow velocity of 15 m/s is selected. As shown in figure 4 on the ground an area behind the aircraft and a part in front of the hangar falls in this definition. Considering the

three-dimensional area of constant velocity, the critical velocities $V \geq 15 \text{ m/s}$ in the environment of the hangar cannot only be found on the ground, but also laterally on the hangar. This effect must be kept in mind when determining security areas.

The flow topology of the flow field close above the ground is shown in figure 5. The streamlines in front of the configuration reflect the wind direction. Furthermore, the streamlines converge in front of the aircraft as a result of the suction of the engines. Behind the aircraft the streamlines are absorbed and accelerated respectively due to the entrainment of the jet. The entrainment effect is caused by the lower static pressure in the jet compared to the ambient pressure and thus the flow enters this low pressure area.

Behind the hangar across from the aircraft side two strong vortices can be found. They are caused by the nearly normally directed wind on the front of the hangar and wake behind it. In contrast on the aircraft side of the hangar both vortices are nearly completely suppressed by the combination of jet- and incoming flow.

Beside the calculation of the flow field the static load on the hangar due to the jet-flow and the wind can be determined from the numerical simulations. From the simulation a maximal static pressure of 104005 Pa can be found on the hangar based on an ambient pressure of 101325 Pa. The hangar-doors should be dimensioned for example with this pressure load. It must be kept in mind, that the pressure inside the hangar may be different from the ambient pressure because of the dynamic pressure in front of the hangar and with it, the load on the hangar-doors can vary.

5 Conclusion

In the present paper aerodynamic questions for the design and the operation of airports are discussed. The problem of jet-blast of aircraft at take-off is shown in detail. This problem can be separated in determining security areas for persons, vehicles and aircrafts and the determination of jet- and wind-loads on buildings and facilities. These aspects have to be considered in the design of buildings close to run or taxiways but likewise by a inspection or modification when new aircraft type (e.g. AIRBUS A380) is introduced.

As an example of the aerodynamic task "jet-blast" the interaction of the engine-jets with a building was shown: As typical obstacle a hangar on the apron area was chosen with jet-blast by a taking-off AIRBUS A380. Further on, cross wind with 20 kts was simulated to show the effect of combined blast- and wind-loads. Among the complete aircraft configuration and in front of a hangar the apron area and coupled with it the ground effect was simulated.

The task jet-blast was addressed by the solution of the Reynolds averaged Navier-Stokes equations using the flow solver DLR TAU. The results for the configuration AIRBUS A380 in front of a hangar the numerical results are discussed and used to determine security areas against jet-blast or the aerodynamic loads on a building.

The application of CFD-methods on aerodynamic questions for the design and the operation of airports is not limited on the application range shown here. In fact,

it can be used for other applications, which cannot be solved with approximative- or handbook methods due to the underlying simplifications.

References

- [1] Kroll, N.; Rossow, C.-C.; Becker, K.; Thiele, F.: *MEGAFLOW - A Numerical Flow Simulation System*. 21st ICAS congress, 1998, Melbourne, 13.09-18.09.1998, ICAS-98-2.7.4, 1998.
- [2] Menter, F.R.: *Zonal Two Equation $k-\omega$ Turbulence Models for Aerodynamic Flows*. AIAA-Paper 93-2906, 1993.
- [3] Kallinderis, Y.: *Hybrid Grids and Their Applications*. Handbook of Grid Generation, CRC Press, Boca Raton / London / New York / Washington, D.C., pp. 25-1 - 25-18, 1999.
- [4] AIRBUS S.A.S: *A380 - Airplane Characteristics For Airport Planning AC (Preliminary Issue)*. AIRBUS S.A.S, Customer Service, Technical Data Support and Services, 31707 Blagnac Cedex, France, September 2003.
- [5] Schlichting, H.; Gersten, K.: *Grenzschichttheorie*. Springer Verlag Berlin, Heidelberg, Auflage 9, 1997.

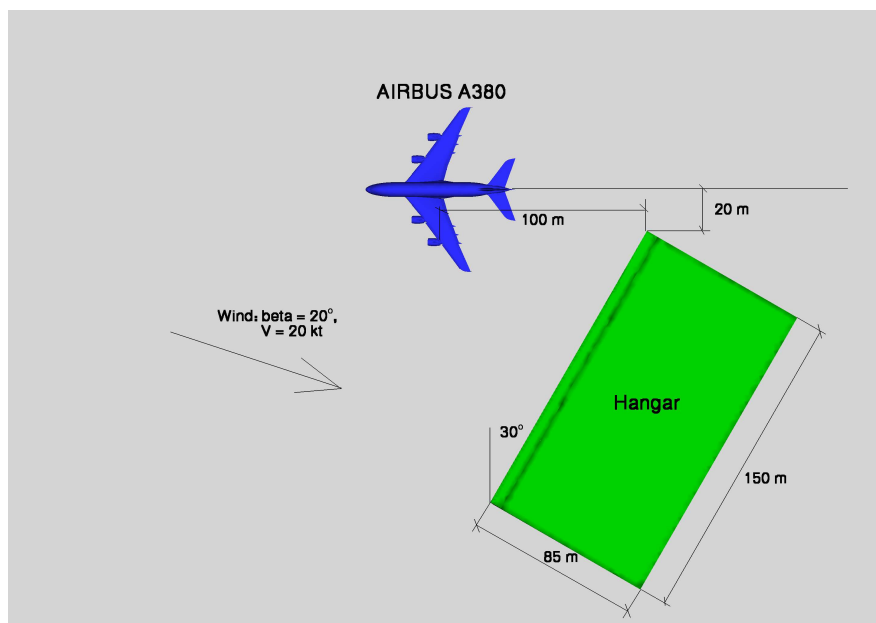


Figure 1 Configuration and alignment: AIRBUS A380 and hangar.

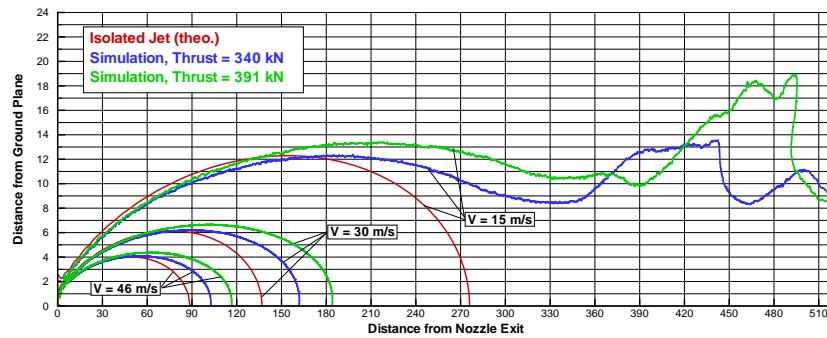


Figure 2 Lines of constant velocity diagram, engine Trent 900, engine-axis on aircraft center-line, comparison of analytical / numerical solution.

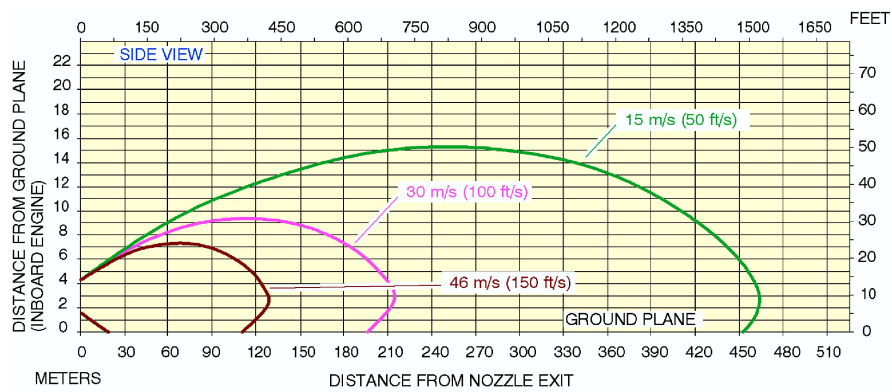


Figure 3 Lines of constant velocity diagram behind engine Trent 977, AIRBUS A380-843F, thrust "max. take-off power", taken from [4].

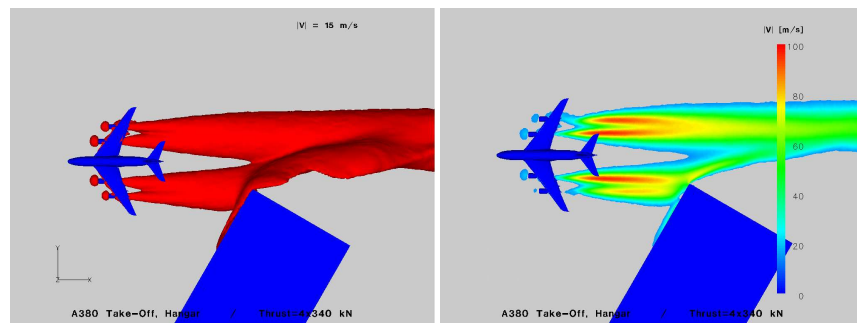


Figure 4 AIRBUS A380 take-off configuration with hangar, thrust 4 x 340 kN, top view, left: area of constant velocity $V = 15 \text{ m/s}$, right: velocity.

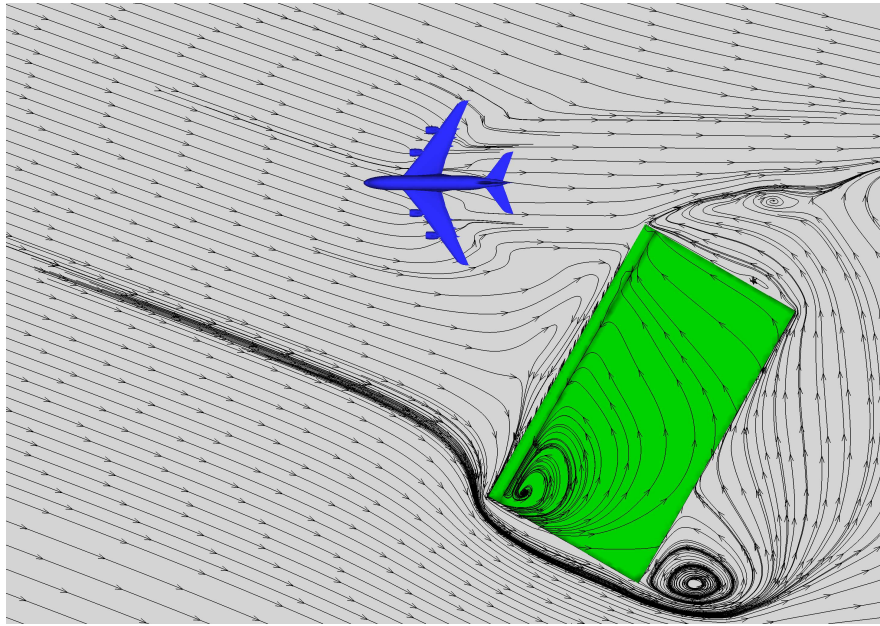


Figure 5 AIRBUS A380 take-off configuration with hangar, thrust 4×340 kN, top view, stream lines.